CrossMark

Seismic interpretation and petrophysical evaluation of SH field, Niger Delta

Oluseun Adetola Sanuade[1] · Adesoji Olumayowa Akanji[2] · Abayomi Adesola Olaojo[3] · Kehinde David Oyeyemi[4]

Abstract Three out of the 14 hydrocarbon-bearing sands (A, B and I) in the 'SH' field onshore Niger Delta which contain bulk of the hydrocarbon reserves in the field were considered as development candidates. Seismic interpretation and petrophysical evaluation of logs of 13 wells were integrated with the aim of verifying and ascertaining the hydrocarbon reserves prior to field development which involves enormous financial commitment. Results show that the field is structurally controlled by sets of northwest–southeast-trending synthetic faults which dip southwest. Hydrocarbon traps at the three sand levels are rollover anticlinal closures that are generally sealed by a major listric fault that demarcated the field into northwest and southeast blocks. The southern fault block is hydrocarbon bearing; wells drilled in the field targeted these closures and encountered a number of stacked hydrocarbon-bearing sand levels. Reservoir-A developed a hanging-wall rollover anticlinal structure sealed by a major listric fault forming a trap with oil–water contact (OWC) of 1222 m TVDSS. Reservoir-B also shows similar structure as reservoir-A, but it is partitioned into two hydrocarbon compartments by a sealing fault; these two compartments have different OWCs. Reservoir-I exhibits similar structure to reservoir-A. The evaluation of the petrophysical characteristics revealed that the reservoirs are of good quality with average net to gross, porosities, water saturation and hydrocarbon saturation ranging from 0.774 to 0.980, 0.220–0.339, 0.133–0.367 and 0.633–0.867, respectively. Variation in the petrophysical parameters and the uncertainty in the reservoir structure of the three reservoirs were considered in calculating range of values of gross rock volume and in-place volume. The study shows oil-in-place volume in the range of 243.83–357.90 MMstb in reservoir-I, whereas reservoir-A contains 148.98–241.14 MMstb, reservoir-B1 31.31–50.36 MMstb and reservoir-B2 67.79–108.98 MMstb of oil. Conclusively, this study has further confirmed the high productivity and commercial viability of the wells within the field of study to be able to adequately compensate for the cost of development.

Keywords Reservoir · 3D seismic · Petrophysics · Hydrocarbon saturation · Fault
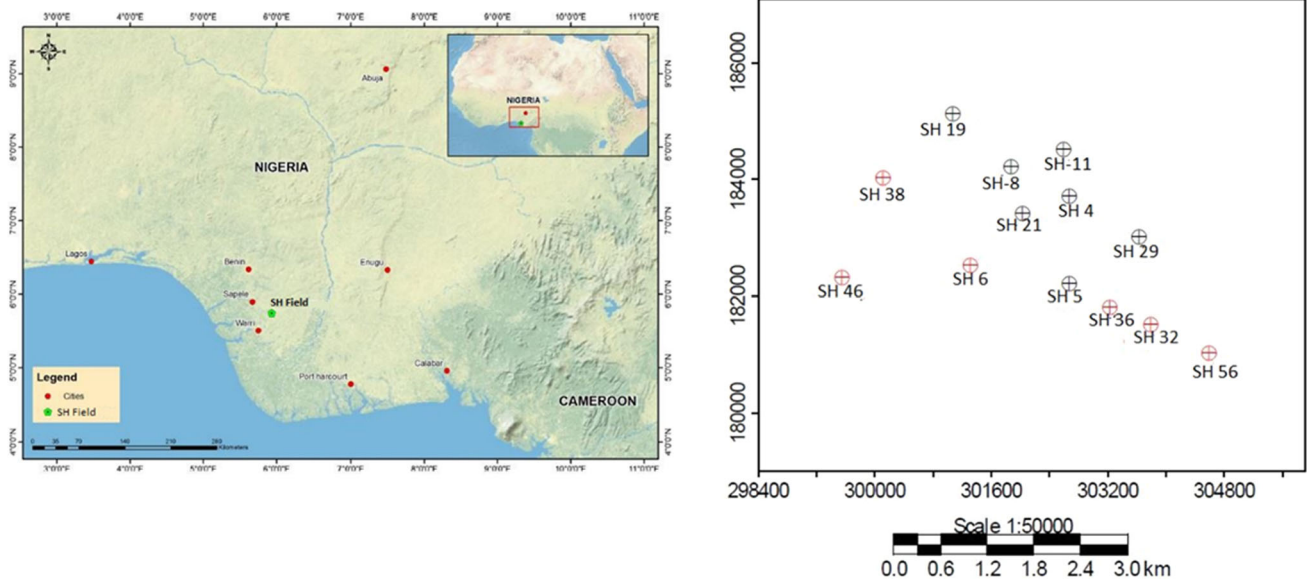
✉ Oluseun Adetola Sanuade
sheunsky@gmail.com

1 Department of Geophysics, Federal University Oye-Ekiti, Oye, Ekiti State, Nigeria

2 Geoexperts Nigeria Ltd, Rockstone Ville Estate, Badore, Ajah, Lagos, Nigeria
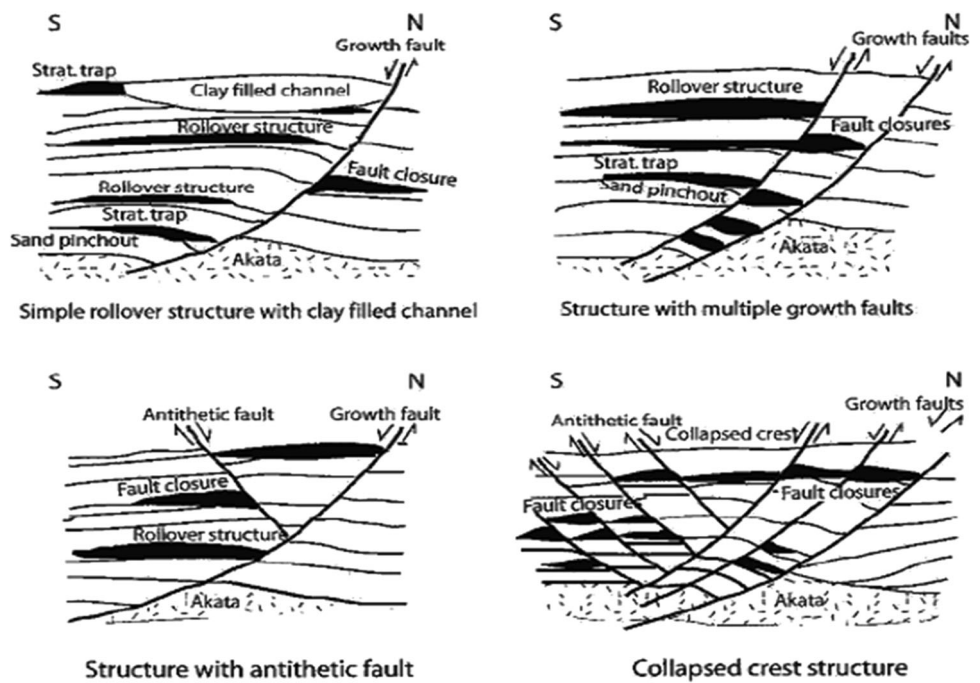
3 Earth Sciences Department, Ajayi Crowther University, Oyo, Nigeria

4 Department of Industrial Physics, Covenant University, Ota, Ogun State, Nigeria

Introduction

Niger Delta province is one of the most prolific basins in Africa typified by six depobelts, notably Offshore, Coastal and Central Swamps, Northern Delta, Greater Ughelli Swamp (Doust and Omatsola 1990). The 'SH' field around the boundary between Coastal and Central Swamps has not been fully explored and exploited to its potential. Although numerous wells have been drilled (Fig. 1) to extract useful information about the field, there still exists some level of uncertainty regarding the reservoir structure and internal anisotropy, fluid properties and hydrocarbon volume.

This research aims to add value to the geology of the field with special interest in estimating the possible oil and

Springer

Fig. 1 Base map of the study area showing well locations in the SH field (modified after Edigbue et al. 2015)

Fig. 2 Niger Delta oil field structures and associated traps (Stacher 1995)

Simple rollover structure with clay filled channel

Structure with multiple growth faults

Structure with antithetic fault

Collapsed crest structure

gas initially in-place considering range of reservoir properties and structural uncertainty. This was achieved by interpreting the 3D seismic data to define the reservoir geometry, evaluating the petrophysical parameters of the reservoirs and determining the lateral extent of the hydrocarbon-bearing zone using the delineated fluid contacts; this helped to estimate the gross rock volume (GRV) and hydrocarbon volume. It has been shown that when 3D seismic data are integrated with well log data, it provides a

powerful tool to determine the structural frame work and estimation of reserves of a field (Futalan et al. 2012; Oyedele et al. 2013; Ihianle et al. 2013; Amigun et al. 2014; Onayemi and Oladele 2014). Therefore, this study entails imaging the subsurface structures, determination of reservoir properties and estimation of volumes for hydrocarbons within reservoirs of the SH field using integrated approach of petrophysical, seismic and volumetric methods.

Geological framework

The clastic wedge of the Niger Delta occurs along a failed arm of a triple junction system which was initially formed in the period of a breakup between the plates of South American and Africa, a process which occurred in the Late Jurassic (Burke et al. 1972; Whiteman 1982). Synrift sediments accumulated during the Cretaceous to Tertiary, with the oldest dated sediments of the Albian age. The thickest successions of synrift marine and marginal marine clastics and carbonates were deposited in a series of transgressive and regressive phases (Doust and Omatsola 1990). The synrift phase finished with basin inversion that occurred in the Late Cretaceous. Renewed subsidence occurred as the continents separated and the sea transgressed the Benue Trough. The Niger Delta clastic wedge prograded into the Gulf of Guinea at an increase rate that was so steady in order to respond to the evolution of these drainage areas and continued basement subsidence. Regression rates increase in the Eocene, with an increasing volume of sediments accumulated since the Oligocene. The movement of deep-seated, over-pressured, ductile, marine shale

Fig. 3 Stratigraphic column showing Formations in the Niger Delta (Tuttle et al. 1999)
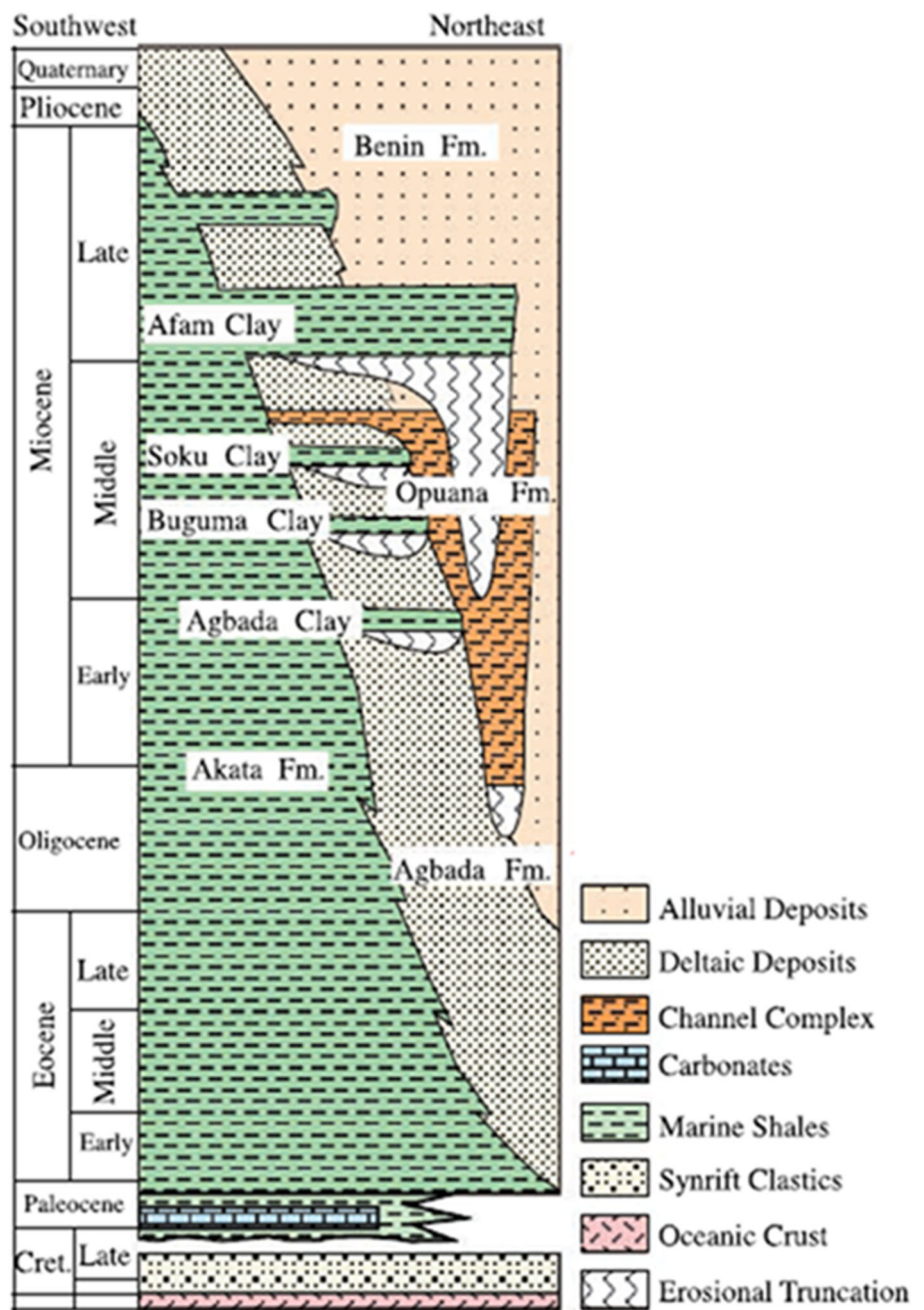
of the Akata Formation within the basin produced normal faults in the basin. The shale tends to have deformed the clastic wedge of the Niger Delta (Doust and Omatsola 1990). Most of these faults are syndepositional and were produced during the progradation of the Delta. The examples of faulting styles in the Niger Delta are shown in Fig. 2.

The clastic Niger Delta has three major lithostratigraphic units which include Akata, Agbada and Benin Formations (Fig. 3); depositional environments range from marine, deltaic to fluvial environments (Weber and Dakoru 1975; Weber 1987).

Akata Formation is about 6400 m thick at the center of the clastic wedge; the lithologies include dark gray shale and silts, having streaks of sand which their origin could be from turbidite flow. The age of this Formation ranges from Paleocene to Recent. This Formation grades vertically into the Agbada Formation with abundant plant remains and micas in the transition zone (Doust and Omatsola 1990).

Agbada Formation extends throughout Niger Delta clastic wedge and has a maximum thickness of about 3962 m. The lithologies of this Formation include alternating sands, silts and shales. Strata in this Formation are believed to have been produced in fluvial–deltaic environment. Agbada Formation ranges from Eocene to Pleistocene in age.

Benin Formation is the top of the clastic wedge Niger Delta. The top of this Formation consists of the recent subaerially exposed delta top surface. The shallow part of Benin Formation is made up of non-marine sands that were deposited in either upper coastal plain or alluvial depositional environments (Doust and Omatsola 1990). Benin Formation ranges from Oligocene to Recent in age (Short and Stauble 1967).

Agbada Formation is the main reservoir in the Niger Delta clastic wedge. The ratio of gas to oil tends to increase toward the south within the depobelts in the Niger Delta. This is because of the complexity in the distribution of hydrocarbons in the basin (Doust and Omatsola 1990).

The source rock in the Niger Delta consists of marine shale of Akata Formation. It could also consist of marine interbedded shales in the Agbada Formation as well as the underlying Cretaceous shale (Evamy et al. 1978; Ekweozor and Okoye 1980; Bustin 1988; Doust and Omatsola 1990). The primary seal rocks are the interbedded shale that occur in the Agbada Formation.

Datasets and methodology

The 3D seismic data and well logs of 13 wells (Table 1) were processed and interpreted using commercial *Petrel* software which is an interactive software to estimate all the parameters needed for the estimation of hydrocarbon volume.

Lithologic units were correlated using the well logs signatures to define the stratigraphy and depositional trends of the rock units. This also helped in describing lateral continuity of the facies as well as the reservoir architecture and compartment. Reservoirs of interest were identified and correlated across the wells to establish the lateral continuity.

The 3D seismic data were processed and interpreted to define the structural frameworks of the SH field. Structures such as synthetic and antithetic faults were mapped out using the reflection discontinuity of geologic events. This was followed by the identification and mapping of horizons of interest on the seismic which corresponds to reservoirs-

Table 1 Well log data available for this study

Wells	CNLLC	ACAL	RHOCN	GR	LLD	SP	LLS	DT
SH-4	√	√	√	√	√	√		
SH-5	√	√	√	√	√	√		
SH-6	√	√		√	√	√	√	
SH-8	√	√	√	√	√	√	√	
SH-11	√	√	√	√	√	√	√	
SH-19	√	√	√	√	√	√	√	
SH-21	√	√	√	√	√	√	√	
SH-29	√	√	√	√	√	√	√	
SH-32	√	√	√	√	√	√	√	
SH-38	√	√	√	√	√	√	√	
SH-46	√	√	√	√	√		√	√
SH-56	√	√	√	√				

ACAL caliper, *LLD* laterolog deep resistivity, *LLS* laterolog shallow resistivity, *CNLLC* neutron porosity, *RHOCN* bulk density, *DT* sonic, *GR* gamma ray)

A, B and I (seismic-to-well tie). Time structure maps of these reservoirs were later generated, and using the available checkshot data and suitable logs, the time maps were converted to top structure maps which were used to calculate the GRV and hydrocarbon volume.

Petrophysical properties of the reservoirs were calculated from the evaluation of the wireline logs of the 13 wells. These parameters include shale volume (V_{shale}), net to gross (NTG), net sand, porosity and water saturation.

Shale volume was calculated using gamma-ray logs by applying 'Larionov tertiary rock' method (Larionov 1969) as shown in Eq. (1):

$$GR_{index} = \frac{GR - GR_{matrix}}{GR_{shale} - GR_{matrix}} \quad (1)$$

Larionov tertiary rock method is given by Eq. (2):

$$V_{sh} = 0.083 \times \left(2^{(3.7 \times GR_{index})} - 1\right) \quad (2)$$

where GR is the gamma-ray (GR) log reading in the zone of interest; GR_{matrix} is the GR log reading in 100% matrix rock; GR_{shale} is the GR log reading in 100% shale; GR_{index} is the gamma-ray index; V_{Sh} is the volume of shale.

Other petrophysical parameters were estimated using Eqs. 3-7.

Porosity (Φ) was estimated from density log using Eq. (3) (Asquith and Krygowski 2004):

$$\emptyset_d = \frac{\rho_{ma} - \rho_b}{\rho_{ma} - \rho_{fl}} \quad (3)$$

where ρ_{ma} = matrix density; ρ_b = density log represents bulk density of the formation; ρ_{fl} = density of the fluid in the formation.

Water saturation was calculated using Eq. (4):

$$\text{Water saturation } S_w = \left(\frac{aR_w}{\emptyset^m R_t}\right)^{1/n} \quad (4)$$

where a = formation factor coefficient; m = cementation exponent; n = saturation exponent; R_w = water resistivity (ohm); R_t = true formation resistivity (ohm); $\emptyset$ = porosity (dec)
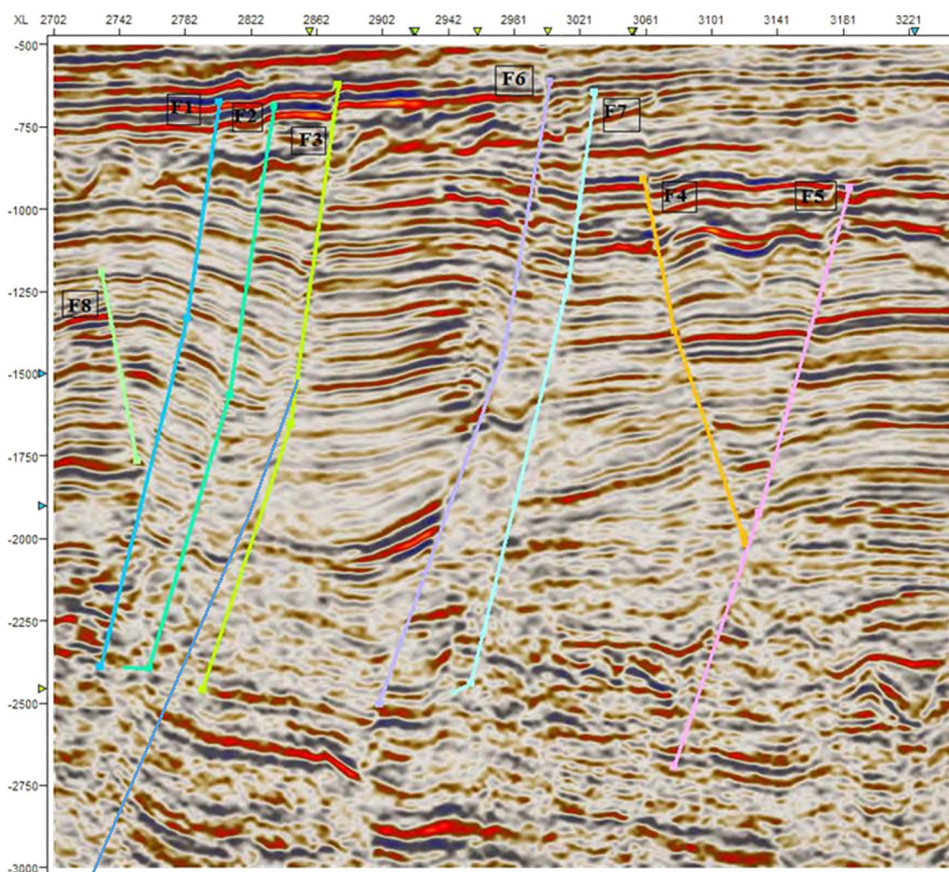
Hydrocarbon saturation is given by Eq. (5):

$$S_h = 1 - S_w \quad (5)$$

Net-to-gross (NTG) ratio was estimated using Eq. (6):

$$\text{Net to Gross,} \quad NTG = \frac{\Sigma(\text{Net Int})}{\Sigma(\text{Gross Int})} \quad (6)$$

where Net Int. is the interval of the net pay section of the reservoir; Gross Int. is the interval of the entire reservoir.

Fig. 4 The major listric faults (F3, F6 and F7) in the field

Fig. 5 Structural interpretation of 'SH' field showing Inline 11,586. It reveals antithetic faults (F4 and F8) and counter-regional faults (F10 and F14)
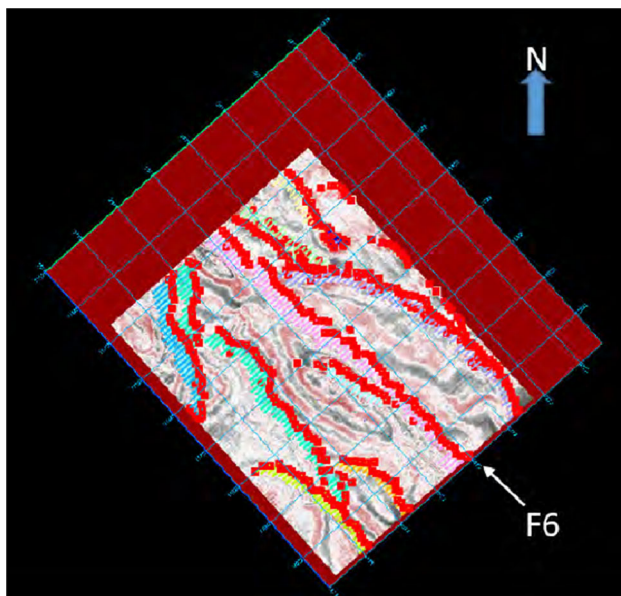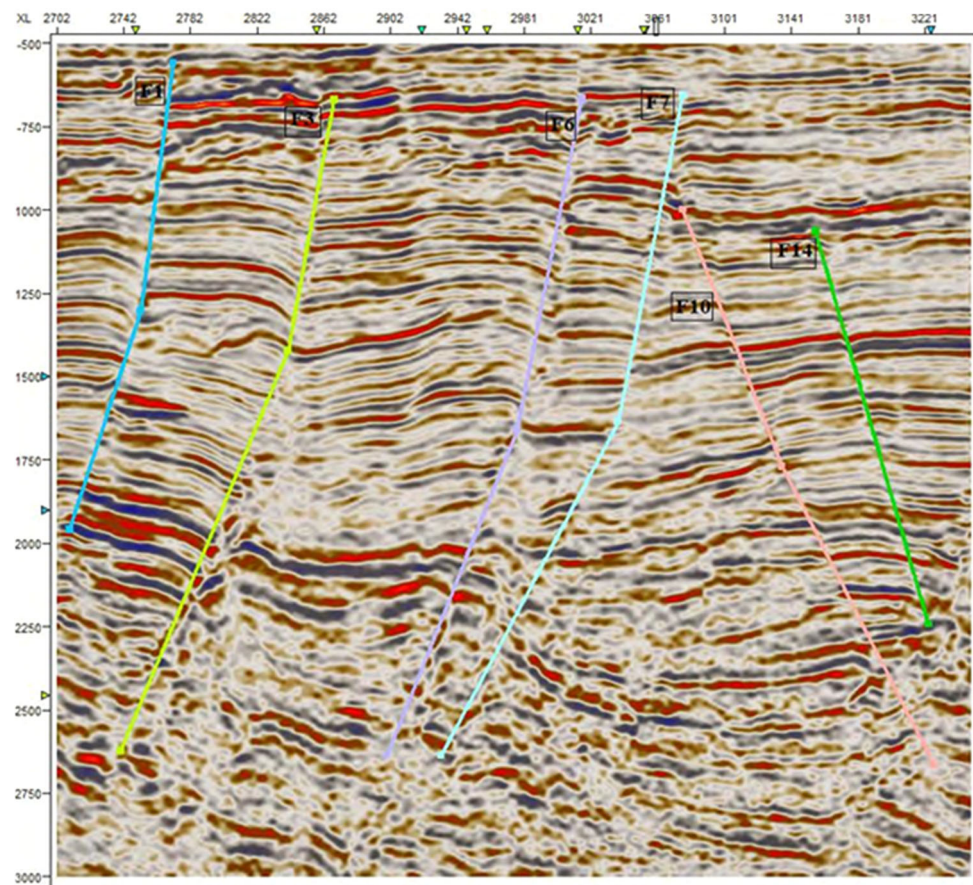
Fig. 6 Time slice at 1500 ms showing NW–SE-trending faults

Deterministic approach was used to estimate hydrocarbon volume (Eq. 7) using input parameters including GRV, porosity, hydrocarbon saturation, formation volume factor (FVF), recovery factor and net pay thickness.

$$STOIIP = \frac{7758 \times GRV \times NTG \times \emptyset \times S_h}{B_o} \qquad (7)$$

where STOIIP = stock-tank oil initially in place expressed in stock-tank barrels, stb, 7758 = conversion factor: acre-ft to barrels, GRV = gross rock volume, expressed in acre-ft, NTG = net-to-gross ratio, expressed as a fraction, $\emptyset$ = average reservoir rock porosity, expressed as a fraction, S_w = average reservoir rock water saturation, expressed as a fraction and B_o = initial oil formation volume factor, having unit of reservoir barrels per stock-tank barrel. Since no PVT or reservoir condition data were provided, a B_o value of 1.135 from close-by field was used.

Results and discussion

Geologic structure and stratigraphy

The field is structurally controlled by sets of synthetic faults (F3, F6, F7, etc.) which trend northwest (NW)–southeast (SE) and dip southwest. There also exist some antithetic faults as shown in Figs. 4 and 5. Structural analysis framework of the study area also reveals NW–SE trending of the faults (Fig. 6). These major faults are

believed to act as conduits for the migration of hydrocarbon from the Akata Formation to the overlying Agbada Formation.

These structures correspond to the general depositional trend in the correlation panels of the shale/sand units of the Agbada and Akata Formations (Fig. 7). The geometry and differential loading of Akata shale probably caused the development of hanging-wall rollover anticlines observed in the SH field; this could serve as hydrocarbon traps.

Hydrocarbon traps at different sand levels in Agbada Formation are generally developed within the hanging-wall rollover anticlinal structures which are generally sealed by Fault F6 (Fig. 6). This major fault appears to demarcate the field into northeast (NE) and southwest (SW) blocks. The southern fault block is hydrocarbon bearing as shown in Fig. 8a, b.

The trap in reservoir-A is a hanging-wall rollover anticlinal structure which is sealed by fault F6 closure and has oil–water contact (OWC) of 1222 m TVDSS (Fig. 8a). Reservoir-B shows similar structure to reservoir-A, but partitioned into two hydrocarbon compartments by a sealing fault; these two compartments have different OWCs. Reservoir-I exhibits similar structure to reservoir-A.

Petrophysical evaluation

Most of the input parameters such as the gross rock volume (GRV), porosity and water saturation are not specific but range in value, thereby creating uncertainty in the volume estimate. Thus, calculation of volumes (GRV, NRV, NPV, OIP and GIP) was done to consider all possible ranges of the input parameters considering the uncertainty in the reservoir structure and petrophysical values. In this research, structural uncertainty was mainly focused on fluid contact. However, other sources of structural uncertainty can arise mainly from fault plane definition, horizon picking, time to depth conversion, etc. The combination of these uncertainties results in ambiguity in the GRV estimates which typically provides the largest uncertainty for calculating hydrocarbon volumes (Shepherd 2009). Uncertainty exists in fluid contacts because most wells that penetrated the hydrocarbon-bearing intervals saw oil and gas at down-to situations, that is, fluid contacts are not known precisely for most reservoir compartments. GRV calculation was therefore done to cover all possible values considering the uncertainty in the fluid contact. For example, if an oil-down-to is observed the spill point depth is used for the calculation of high-case GRV.
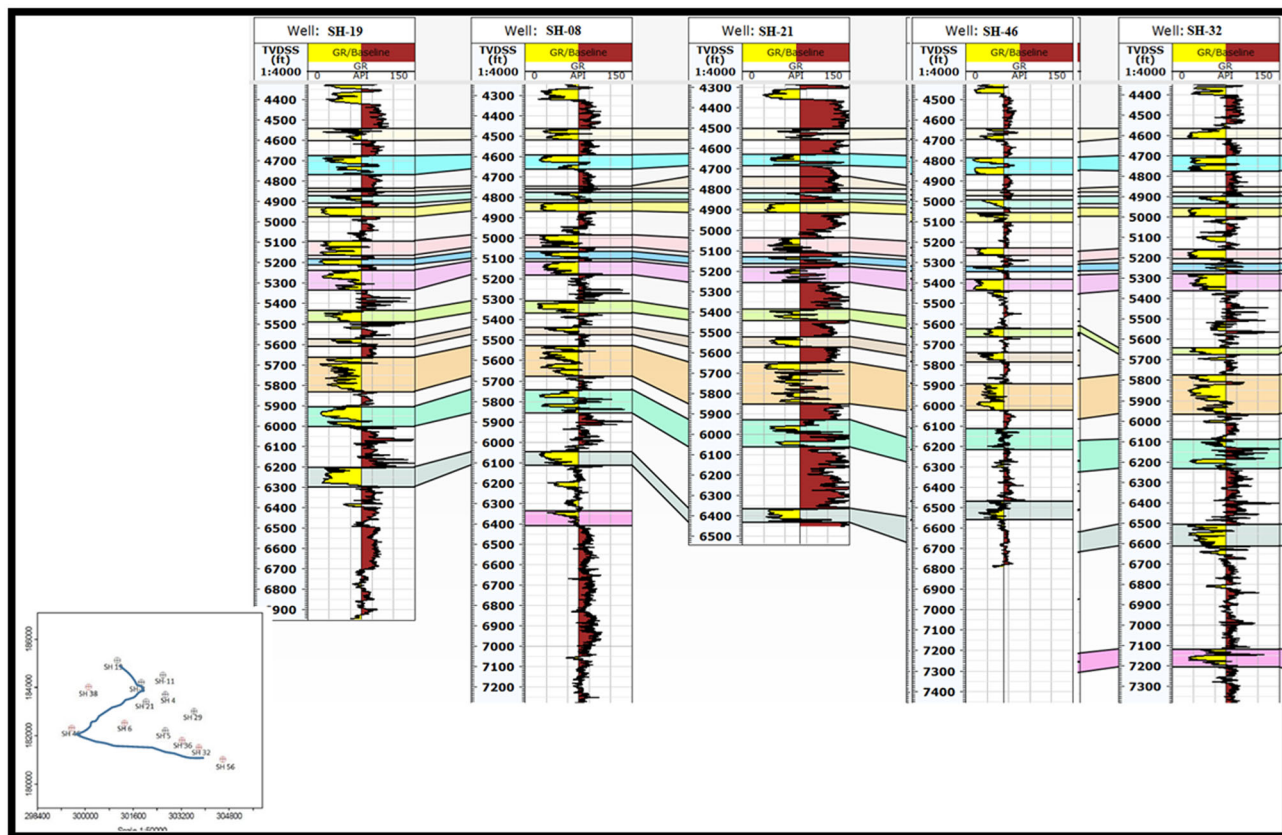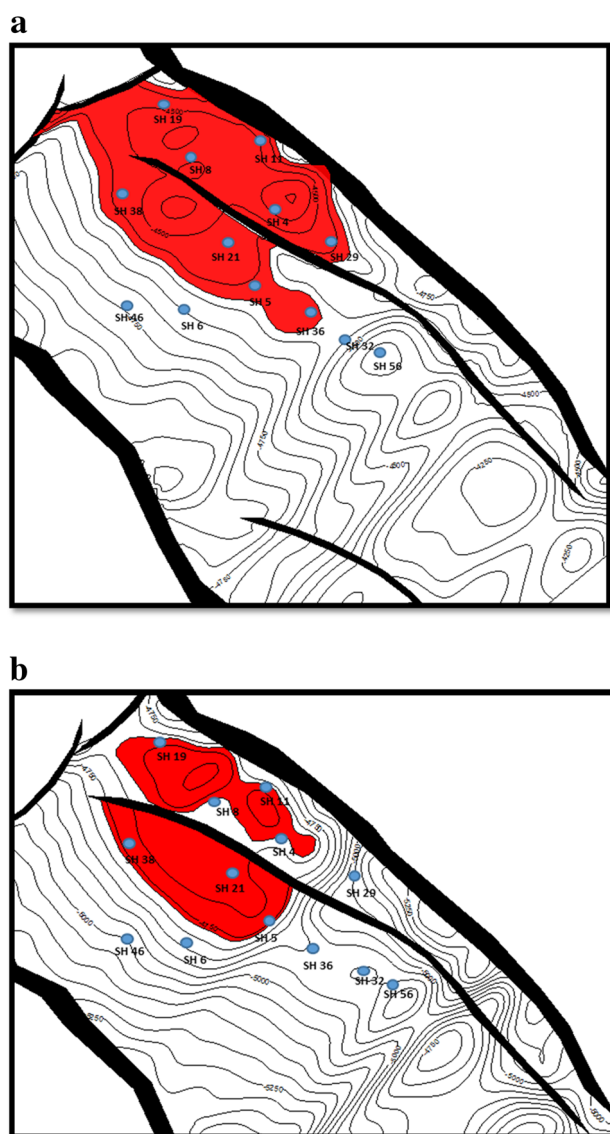

Fig. 7 Correlation panel showing the continuity of the sand and shale units

a

b

Fig. 8 a Top structure map of reservoir-A. **b** Reservoir-B depth structure map

Petrophysical properties of the reservoirs are summarized in Table 2. Reservoirs-A, B and I are relatively clean with NTG between 0.774 and 0.980 and net thickness within 31 ft to 77 ft. Porosity (ϕ) values are within 0.220 and 0.339, water saturation (S_w) from 0.133 to 0.367 and hydrocarbon saturation (S_h) 0.633 and 0.867.

The area covered hydrocarbon-bearing zone was estimated from the top structure maps and used to estimate GRV and volume of hydrocarbon in place as given in Table 3. Considering the range of uncertainty in the structure, the estimated hydrocarbon volumes were calculated to cover all possible values of the input parameter; as a result, the estimates were grouped into low, medium and high case to cover the range of possibility of the petrophysical properties of reservoir and uncertainty in the reservoir structure. Reservoir-A has a STOIIP of 148.98 MMstb for the low case, 200.85 MMstb for the medium case and 241.14 MMstb for the high case. B1 compartment of reservoir-B has 31.31 MMstb for the low case, 42.14 MMstb for the medium case and 50.36 MMstb for the high case, whereas B2 compartment has 67.79 MMstb for the low case, 91.20 MMstb for the medium case and 108.89 MMstb for the high case. Reservoir-I on the other hand has STOIIP of 234.83 and 108.89 MMstb for the low case, 315.69 and 108.89 MMstb for the medium case and 357.90 and 108.89 MMstb for the high case (Table 3). The range of STOIIP (MMstb) for reservoirs-A, B and I is shown in Fig. 9. This chart shows that huge uncertainty exists in the volume estimate for reservoir-I than for A and B and also contains much more reserves than reservoirs-A and B.

This study shows that reservoirs-A, B and I cumulatively have STOIIP ranging between 482.91 MMstb and 758.36 MMstb and at assumed recoverable factor of 30%, the oil recoverable reserves range between 144.87 MMstb and 227.51 MMstb. The low-case value is substantial enough to embark on field development.

Conclusions

The structural interpretation of the seismic data reveals three major listric faults that trends northwest (NW)–southeast (SE) and dip toward the southwest. There are also several antithetic faults in the 'SH' field. This trend agrees with the typical structural style in the Niger Delta Province. A review of the reservoir characteristics showed that they vary widely across the

Table 2 Summary of the petrophysical parameters used for the volumetric

Reservoirs	Porosity			Sw			NTG			Average HC column (ft)
	Minimum	Mean	Maximum	Minimum	Mean	Maximum	Minimum	Mean	Maximum	
A	0.243	0.299	0.342	0.247	0.32	0.39	0.848	0.926	0.985	35.15
B	0.22	0.278	0.315	0.207	0.284	0.367	0.825	0.876	0.95	68.27
I	0.298	0.313	0.329	0.197	0.231	0.298	0.774	0.931	1	202

Table 3 Volume of hydrocarbon in place of the reservoirs

Reservoirs	Area (acre)			Boi	STOIIP (MMstb)		
	Low	Medium	High		Low case	Medium case	High case
A	2452.239	2724.71	2997.181	1.135	148.9762	200.8484	241.136
B1	663.239	736.932	810.625	1.135	31.30646	42.14087	50.35841
B2	495.461	550.215	605.237	1.135	67.78704	91.19724	108.981
I	1783.42	1981.578	2179.736	1.135	234.831	315.6898	357.9035

Fig. 9 Range of STOIIP (MMstb) for reservoirs-A, B and I
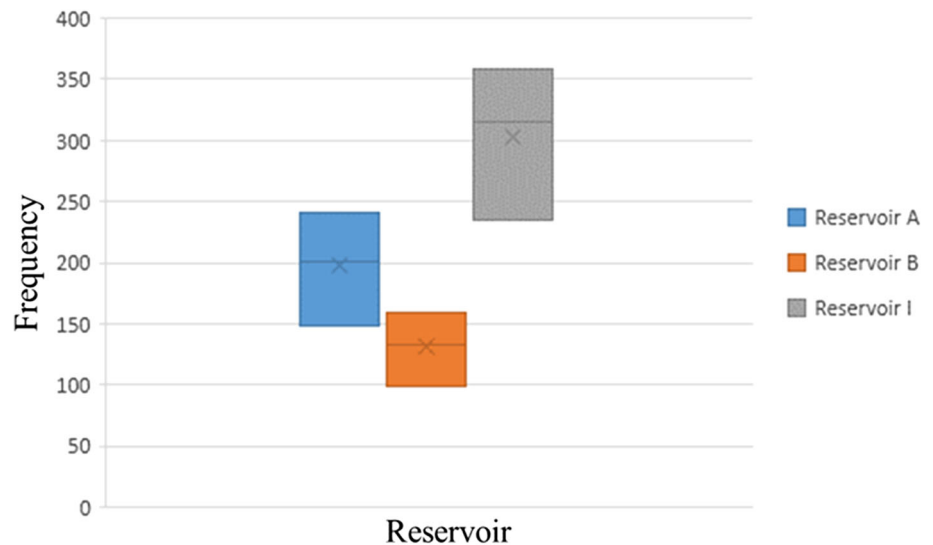
field. Petrophysical evaluation shows that reservoirs are generally of good quality with average porosities between 0.220 and 0.339 and hydrocarbon saturation averaging between 0.633 and 0.867. Oil-in-place volume within the three reservoirs is estimated to range between 482.91 MMstb and 758.36 MMstb. At 30% recovery, the potential recoverable reserves are 144.87 MMstb for the low case and 227.51 MMstb for the high case. Results of this study have shown the efficacy of integrating seismic interpretation and petrophysical evaluation in weighing hydrocarbon potential of reservoirs and also to reach development decisions. The need to optimize production from the field has led to detailed description of the reservoirs in terms of structure and hydrocarbon volume. Besides, the result will help to plan the development approach and forecast production and will also be helpful in providing very effective reservoir management strategy throughout the life of the field. Further, studies such as AVO/AVA analysis and sequence stratigraphy could greatly enhance a proper evaluation and reduce the uncertainty especially in the petrophysical characteristics of the reservoirs. It would also help to optimally position development wells for optimum production.

References

Amigun JO, Adewoye O, Olowolafe T, Okwoli E (2014) Well logs-3D seismic sequence stratigraphy evaluation of "holu" field, Niger Delta, Nigeria. Int J Sci Technol 4:26–36

Asquith G, Krygowski D (2004) AAPG methods in exploration, No. 16: basic well log analysis. 2nd edn. The American Association of Petroleum Geologists, pp 240–244 [**with sections by Steven Henderson and Neil Hurley**]

Burke RC, Desauvagie TFJ, Whiteman AJ (1972) Geological history of the Benue Valley and adjacent areas. University Press, Ibadan

Bustin R (1988) Sedimentology and characteristics of dispersed organic matter in tertiary Niger delta: origin of source rocks in a deltaic environment. AAPG Bull 72:277–298

Doust H, Omatsola M (1990) Petroleum geology of the Niger delta. Geological Society, London, Special Publications, 50:365–365

Edigbue P, Olowokere MT, Adetokunbo P, Jegede E (2015) Integration of sequence stratigraphy and geostatistics in 3-D reservoir modeling: a case study of Otumara field, onshore Niger Delta. Arab J Geosci 8(10):8615–8631

Ekweozor CM, Okoye NV (1980) Petroleum source-bed evaluation of Tertiary Niger Delta. AAPG Bull 64:1251–1259

Evamy B, Haremboure J, Kamerling P, Knaap W, Molloy F, Rowlands P (1978) Hydrocarbon habitat of tertiary Niger delta. AAPG Bull 62:1–39

Futalan K, Mitchell A, Amos K, Backe G (2012) Seismic facies analysis and structural interpretation of the Sandakan sub-basin, Sulu Sea, Philippines. AAPG International Conference and Exhibition (Singapore), www.searchanddiscovery.com/pdfz/documents/2012/302 54futalan/ndx_futalan.pdf.html

Ihianle OE, Alile OM, Azi SO, Airen JO, Osuoji OU (2013) Three dimensional seismic/well logs and structural interpretation over 'X-Y' field in the Niger Delta area of Nigeria. Sci Technol 3(2):47–54

Larionov VV (1969) Borehole radiometry: Moscow, U.S.S.R., Nedra

Onayemi J, Oladele S (2014) Analysis of facies and depositional systems of "Ray" field, on shore Niger Delta basin, Nigeria. SEG Annual Meeting, www.onepetro.org/conference-paper/SEG–2014-0019

Oyedele K, Ogagarue D, Mohammed D (2013) Integration of 3D seismic and well log data in the optimal reservoir characterization of "Emi" field, off shore Niger delta oil province, Nigeria. Am J Sci Ind Res 4:11–21

Shepherd M (2009) The reservoir framework. In: Shepherd M (ed) Oil field production geology: AAPG Memoir 91, pp 81–92

Short K, Stauble A (1967) Outline of geology of Niger delta. AAPG Bull 51:761–779

Stacher P (1995) Present understanding of the Niger delta hydrocarbon habitat: Geology of Deltas. AA Balkema, Rotterdam, pp 257–267

Tuttle ML, Charpentier RR, Brownfield ME (1999) The Niger delta petroleum system: Niger delta province, Nigeria, Cameroon, and Equatorial Guinea, Africa: US Department of the Interior, US Geological Survey

Weber KJ (1987) Hydrocarbon distribution pattern in Nigerian growth fault structures controlled by structural style and stratigraphy. J Petrol Sci Eng 1(1–12):1987

Weber KJ, Dakoru EM (1975) Petroleum geology of the Niger delta: proceedings of the Ninth World Petroleum Congress, v. 2, Geology, London, Applied Science Publishers, Ltd., pp 210–221

Whiteman A (1982) Nigeria: its Petroleum Geology, Resources and Potential. Graham and Trotman, London